**Article:**

Jayathilaka, P, Indraratna, B and Heitor, A orcid.org/0000-0002-2346-8250 (2021) Influence of Salinity-Based Osmotic Suction on the Shear Strength of a Compacted Clay. International Journal of Geomechanics, 21 (5). 04021041. ISSN 1532-3641

https://doi.org/10.1061/(ASCE)GM.1943-5622.0001988

# INFLUENCEOFSALINITY BASED OSMOTIC SUCTION ON THE SHEAR STRENGTH OF A COMPACTED CLAY

**PubuduJayathilaka**

PhD student,

Centre for Geomechanics and Railway Engineering, University of Wollongong,

NSW 2522, Australia

**Buddhima Indraratna**[1]

Distinguished Professor of Civil Engineering,

Director, Transport Research Centre, University of Technology Sydney, Australia

Formerly, Director, Australian Research Council (ARC) Industrial Transformation Training Centre, ITTC-Rail, University of Wollongong, Australia

**Ana Heitor**

School of Civil Engineering, University of Leeds, Leeds, UK

Formerly Centre for Geomechanics and Railway Engineering, University of Wollongong,

NSW 2522, Australia

Words: 6584; Figures: 14

Submitted to:

[1]Corresponding author: Prof Buddhima Indraratna

Email: buddhima.indraratna@uts.edu.au

ABSTRACT

As most previous studies have neglected the positive influence of salinity (osmotic suction) on most coastal soils in Australia, the design of transport infrastructure involving these soils have often been overly conservative. In this study, a laboratory approach based on direct shear testing is explained to determine the stress-strain behaviour of compacted coastal silty clay (CL) at different levels of osmotic suction generated by varying salinity (NaCl) concentrations. A broad data set for a total of 147 direct shear tests conducted on remoulded and re-compacted test specimens at seven different initial matric suction conditions is analysed to develop a semi-empirical model that captures the effect of osmotic suction on the soil shear strength. The results suggest that greater the initial matric suction is the more pronounced will be the role of osmotic suction. The proposed semi-empirical model is governed by an electrical conductivity relationship with the osmotic suction generated by soil salinity. A new parameter $\chi_2$ is introduced to quantify the role of soil salinityon the apparent soil shear strength corresponding to different levels of osmotic suction. When this novel relationship is coupled with the conventional matric suction theory, the overall unsaturated shear strength of a saline soil can be properly evaluated, as proven by the close proximity of the predictions to the measurements.



**Keywords:**Unsaturated, matric suction, osmotic suction, shear stress

## INTRODUCTION

Most types of civil infrastructure are built on and remainunder unsaturated conditions for most of their service life; therefore, the stability of these structures with increased loading in the future will depend on the actual shear strength of the foundation soil (sub-grade). Especially in notably saline soils prevalent along the coastal belt of Australia, neglecting the benefits of salinity-based osmotic suction can lead to undue design conservatism. Past studies have shown that the magnitudes of both matric and osmotic suction influence the shear strength of a natural or compacted soil (Graham et al., 1992, Barbour and Fredlund, 1989). However, while the effect of matric suction on the shear strength is well established through comprehensive testing and analysis (Khalili, 2018, Vanapalli et al., 1996, Bishop, 1960, Khalili et al., 2004), only a limited number of studies have focussed on the role of osmotic suction. For instance, Tiwari and Ajmera (2014), Xu (2019), and Di Maio and Scaringi (2016)verified the corresponding increase in soil shear strength as the osmotic suction is increased. Fredlund et al. (2012) pointed out that osmotic suction would have greater influence at higher values of matric suction, hence a key reason why the authors in the current study have investigated the role of osmotic suction at different levels of matric suction for a coastal saline soil. Elsewhere in relation to plant morphology, Pathirage et al. (2017) and Jayathilaka et al. (2019) have pointed out that the variations of soil osmotic suction can also be associated with the nutrient uptake by roots; this effect is not considered in this study.

Osmotic suction stems from the salts dissolved in the pore water of a soil, and particularly in coastal areas salinity is significantly increased by sodium chloride ($NaCl$) that is transported and deposited in inland areas over the geological time domain, i.e. in some instances, even several thousands of km away from the present-day marine boundary. Arora (2017) reports that around 400 million hectares, which is more than 6% of the total landmass of the earth can be categorised as saline, while in Australia alone, about 30% of its landmass is considered to be saline (Rengasamy, 2006).

The soil strength is influenced by the degree of saturation, the presence of various chemical compounds, the overburden and confining ground pressure, and the fabric of the soil and pore water conditions that also influence the inter-particle behaviour(Murray and Sivakumar, 2010). The osmotic suction induced by variations in pore water salinity can induce inter-particle forces, e.g. van der Waal attraction forces, electrostatic repulsive forces, and surface hydration forces (Li et al., 2013). While some of these stress components can help to reduce potential swelling (Rao and Thyagaraj, 2007), as the osmotic suction changes, the hydraulic and mechanical properties of a compacted soil also contribute to the thinning of the diffusive double layer (DDL), cause the particles to coagulate, and increase the effective stress (Di Maio et al., 2004). While the effective pressure acting on clay particles can be described for instance by Derjaguin-Landau-Verwey-Overbeek (DLVO) theory of stability (Liang et al., 2007), determining the magnitudes of these inter-particle forces through accurate measurements is still a challenge(Fredlund et al., 2012). Electrical conductivity is widely used in geophysical applications (Shevnin et al., 2010, Jiao-Jun et al., 2007, Shah and Singh, 2004), while its ability to corroborate with matric suction (Hen-Jones et al., 2014, Piegari and Maio, 2013) and osmotic suction (Adam et al., 2012, Read and Cameron, 1979) has been widely tested and discussed. Nevertheless, the combination of electrical conductivity and osmotic suction to predict the soil shear strength is still at infancy.

In view of the above, a novel osmotic stress parameter ($\chi_2$) is introduced in this paper to determine the stress induced by changes in osmotic suction attributed to different salt concentrations in the pore water. The role that osmotic suction plays in the shear strength of a soil compacted at different levels of matric suction is then investigated through a series of direct shear tests.

## OSMOTIC STRESS PARAMETER

A new shear strength model which can capture the influence of both the matric and osmotic suction on the shear strength is introduced in this paper. Here, the shear strength of the soil with pore water salinity can be partially related to the saturated shear strength parameters based on the traditional effective cohesion ($c'$) and effective friction angle ($\phi'$). In addition, instead of the effective stress parameter ($\chi_1$) proposed by Khabbaz and Khalili (1998), a revised osmotic stress parameter ($\chi_2$) that depends on the level of salinity in pore water is introduced as follows:

$$\sigma_{net} = (\sigma_N - u_a) + \chi_1(u_a - u_w) + \chi_2\pi \tag{1}$$

In the above, the term $(\sigma_N - u_a)$ is the effective normal stress, $\sigma_N$ is the total normal stress, the parameter $\chi_1 = \left(\frac{u_a - u_w}{AEV}\right)^{-0.55}$ is the effective stress parameter that depends on the matric suction, the term $(u_a - u_w)$ is the matric suction, $u_a$ is the pore air pressure, $u_w$ is the pore water pressure, $AEV$ is the air entry value, and $\pi$ is the osmotic suction.

Equation (1) conforms with the postulate that the inter-particle physio-chemical stresses can be superimposed directly to the classical effective stress concept (Lu & Likos 2006; Rao & Thyagaraj 2007). Also as proposed earlier by Lu and Likos (2006), the net inter-particle contact forces due to physico-chemical effects can be determined by the summation of chemical cementation (bond stresses), van der Waals attraction forces, and the repulsion forces of DDL. Therefore, by characterising $\chi_2$ in terms of inter-particle contact, the relevant forces are more realistically acknowledged, but as noted by Fredlund et al. (2012), the methods of determining or measuring the correct magnitude of the aforementioned inter-particle contact forces remains a challenge.

## EXPERIMENTAL DETERMINATION OF $\chi_2$

According to Khabbaz and Khalili (1998), the shear strength of unsaturated soil can be estimated in terms of the effective normal stress $(\sigma_N - u_a)$ and matric suction $(u_a - u_w)$:

$$\tau'_U = [(\sigma_N - u_a) + \chi_1(u_a - u_w)] \tan\phi' + c' \quad (2)$$

Where, $\tau'_U$ is the unsaturated shear strength, $\sigma_N$ is the total normal stress, $u_a$ is the pore air pressure, $u_w$ is the pore water pressure, $\chi_1$ is the effective stress parameter that depends on the matric suction, $\phi'$ is the effective friction angle, and $c'$ is the effective cohesion component. Since the effective stress generated in an unsaturated soil element is defined by considering the net stress constituting the pore water and pore air pressures, pore water salinity (hence, the matric and osmotic suction, and physio-chemical pressure), it is assumed that the shear strength parameters $c'$ and $\phi'$ of saturated soil are independent of the matric suction (Khabbaz and Khalili, 1998) and of the salinity-based osmotic suction (Lu and Likos, 2006). Combining these concepts in a mathematical sense, a refined shear strength model for unsaturated-osmotic conditions is now defined by the following expression:

$$\tau'_{US} = [(\sigma_N - u_a) + \chi_1(u_a - u_w) + \chi_2\pi] \tan\phi' + c' \quad (3)$$

Where $\tau'_{US}$ is the shear strength of osmotically induced unsaturated soil.The difference between Equations (2) and (3) is given by the osmotic suction component as follows:

$$\tau'_{US} - \tau'_U = \chi_2\pi \tan\phi' \quad (4)$$

Hence, according to Equation (4), the only unknown parameter $\chi_2$ can be estimated.

$$\chi_2 = \frac{\tau'_{US} - \tau'_{U}}{\pi \tan \phi'} \tag{5}$$

RELATIONSHIP BETWEEN $\chi_2$ AND THE ELECTRICAL CONDUCTIVITY RATIO

Electrical conductivity is a function of the salt concentration so it can also be considered as a function of osmotic suction (Abedi-Koupai and Mehdizadeh, 2007). To investigate the behaviour of $\chi_2$ the electrical conductivity of soil is used as an additional influencing factor. A semi-empirical model parameter (i.e. $\chi_2$) is introduced based on the experimental results. In this model, ECR is used to represent the change of salinity in pore water and $S_r$ is used to incorporate the influence of the degree of saturation.

$$\chi_2 \begin{cases} = 0 & \pi = 0 \\ = \dfrac{a}{S_r^c}\left(1 - \exp\left(-b(ECR)\right)\right) & \pi \neq 0 \end{cases} \tag{6}$$

In the above, the electrical conductivity ratio $(ECR) = \frac{\Delta EC}{EC_i}$, $\Delta EC = (EC - EC_i)$, $EC$ is the electrical conductivity of the saturated soil for a given salt concentration in pore water, $EC_i$ is the initial electrical conductivity of saturated soil remoulded with distilled water, $S_r$ is the degree of saturation, and $a, b$ and $c$ are empirical coefficients from the regression analysis of experimental results.

The sensitivity of $\chi_2$ depends mainly on the above three experimental coefficients, and their influence on $\chi_2$ is shown in Fig. 1. The coefficient $a$ increases to the maximum of $\chi_2$, however, coefficient $b$ does not influence the maximum value of $\chi_2$, but rather contributes to the lowest value of ECR having the maximum $\chi_2$. The maximum theoretical value of $\chi_2$ can then be calculated from Equation (7).

$$\chi_{2_{max}} = \left(\frac{a}{S_r^c}\right) \qquad (7)$$

According to Equation (7), $\chi_{2_{max}}$ does not depend on the electrical conductivity ratio (ECR), although $\chi_2$ is a function of ECR. This is further validated by Fig. 1(d) which shows the distribution of $\chi_2$ with respect to ECR for different $\frac{a}{S_r^c}$ratios. According to Fig. 2, the distribution of $\chi_{2_{max}}$ with respect to the empirical coefficient *c* is linear at higher degrees of saturation, but the distribution of $\chi_{2_{max}}$ becomes exponential as the degree of saturation decreases. Therefore, at higher matric suctions (i.e. lower degree of saturation), the influence of $\chi_2$ will be significant compared to that of a soil having a lower soil matric suction (high degree of saturation).

The minimum ECR value where $\chi_2$ reaches its maximum and the critical ECR (i.e. $ECR_C$) depends on the empirical coefficient *b*[Fig. 1(b)], therefore, $\chi_{2_{max}}$ increases as the soil approaches a dry state. The distribution of $ECR_C$ with respect to the empirical coefficient *b* for different levels of saturationis shown in Fig. 3. Here, for every degree of saturation, the $ECR_C$ decreases as the coefficient *b*increases, following a power decay function. For example, under fully saturated conditions ($S_r$ = 1), when the coefficient *b* increases from 0.01 to 0.08, the $ECR_C$ decreases from 750 to 125.

MATERIALS AND TESTING PROGRAM

**Soil type and preliminary testing**

The soil samples were obtained from the coastal region of Wollongong (85 km south of Sydney). The particle size distribution (AS1289.3.6.1) indicates it consists of sand (48%), silt (36%), and clay (16%) particles (Fig. 4). The liquid and plastic limits (AS1289.3.1.1 and AS1289.3.2.1) are 46.8% and 27.7%, so this soil can be classified as a sandy, silty clay of low plasticity, CL, based on the ASTM Unified soil classification (ASTM D2487 2010). The modified Proctor compaction characteristics according to AS1289.5.1.1 enabled a maximum dry density (MDD) of 15.58 kN/$m^3$at an optimum moisture content of 27.2%, and a specific gravity of the soil was determined to be 2.62 (AS1289.3.5.2).

The matric suction of the compacted soil was measured using the contact method and Whatman No 42 filter paper approach (ASTM D5298-03). The soil water retention data was only measured for test specimens remoulded with distilled and de-aired water. Thirteen different samples were prepared at different moisture contents, and then they were air sealed and stored for seven days in a temperature and humidity controlled room (20±2$^o$C, 30%RH) to attain moisture equilibrium. The samples were then compacted into a 50mm diameter cylindrical mould to 85% of MDD. Fig. 5 shows the soil water retention curve calibrated with the Van Genuchten (1980) model (Van Genuchten 1980) withbest-fit parameters: m=0.306, n=1.44, and α=0.008.

Although, the osmotic suction can be theoretically calculated according van Hoff's equation ($\pi = \upsilon R^{*}TC$), where $\pi$ is the osmotic suction, $R^{*}$ is the universal gas constant, $T$ is the absolute temperature, $\upsilon$ is the valency, and $C$ is the ion concentration. In this study, the actual osmotic suction was measured using a WP4 Dew Point Potentiometer. Crystallised NaCl were mixed with distilled water to prepare a solution with the desired salt concentrations. Although the soil contains constant ion content, the pore water salinity is likely to increase due to soil moisture decrease (i.e. caused by a rise in global temperature induced by climate change). Therefore, it is appropriate to consider a broader range of salinity values. Therefore, seven soil samples were fully saturated with solutions having NaCl concentrations of 0.0, 0.2, 0.4, 0.6, 0.8, 1.0 and 2.0 mol/L, where the maximum salinity of the studied soil was three times more than the maximum salinity of seawater (i.e. 35 g/L). Also, the inherent salt content of the soil specimen was determined by X-Ray diffraction (XRD) as less than 0.1%. Therefore, for this study, the contribution of inherent salt content could be assumed as negligible. The samples were then fully sealed and stored in a temperature and humidity controlled room (20±2$^{o}$C, 30% RH) for another 24 hours. Although the WP4C Dew Point Potentiometer could be used to measure total suction, in this study, as the seven test specimens remained fully saturated the matric suction was 0 kPa. On this basis, the measured total suction was assumed to be equal to the osmotic suction of the specimen. The moisture equilibrated samples were placed into clean plastic cups and tested with a WP4C Dew Point Potentiometer (range 0 to 300 MPa). The measured values of osmotic suction are summarised in Table 1.

Seven samples saturated with different pore water salinities were prepared and stored in the temperature and humidity-controlled room for 24 hours. These moisture equilibrated samples were then compacted to a dry density of 13.24 kN/m$^3$ (85% of MDD) and then placed into a standard electrical resistivity measuring box having dimensions of 38 x 101.5 x 152.3 mm. The electrical resistivity was measured using a Tinker and Rasor SR-2 soil resistivity meter (±0.1 Ωcm accuracy) and then converted to electrical conductivity (=1/Electrical resistivity).

The distribution of electrical conductivity with the pore water saline concentration is summarised in Fig. 6.

**Direct shear test**

Seven different solutions with different osmotic suctions were prepared by mixing the relevant amount of commercially available crystallised NaCl with distilled water; only NaCl was used to mimic the conditions of coastal soils.  Different levels of initial matric suction (0, 25, 100, 200, 500, 1000 and 1500 kPa) were targeted by controlling the moisture content of the specimens. The required amount of water and the relevant salt concentration were added to the soil, and then the mixture was left in the temperature and humidity-controlled room for seven days for chemical and moisture equilibration. The samples were then compacted in a 60×60×40 mm shear box chamber to attain 85% of MDD, and then stored in the temperature and humidity-controlled room for two more days.

A motor-driven direct shear box where the specimen carriage travels on roller bearings was used to maintain a constant rate of horizontal displacement of 0.006 mm/min. A load cell and two LVDT transducers accurate within ±0.001 kN,±0.001mm and ±0.001 mm, respectively, were used to determine the horizontal shear force, vertical displacement, and horizontal displacement.  A lever arm loading system (beam ratio 10:1) was used to apply a vertical load by a top cap modified to accommodate a miniature pore water pressure transducer, so that any variations in the matric suction could be monitored during shearing. An in-house coded program with Lab VIEW software complemented by a National Instruments card (NI USB-6009) with eight input channels was used to acquire data every 60 seconds. A schematic diagram and few images of the actual test set up of the direct shear box are given in Fig. 7.

Apart from those specimens with a matric suction of 0 kPa (fully saturated conditions), direct shear tests were carried out at different levels of matric suction under constant water (CW) contents. For fully saturated experiments where the matric suction = 0 kPa, the compacted specimens were fully submerged in the desired saline solution for 24 h before shearing to attain moisture and chemical equilibration. To ensure CW conditions, evaporation from the soil specimen had to be minimised so the compression and shearing stages of the direct shear tests could occur within a temperature and humidity-controlled environment. The top and bottom surfaces of all test specimens were covered with a 1mm thick film of polyethylene to minimise evaporation. Moreover, the space between the top and bottom sliding halves, and any other gaps between the top cap and bottom plate were sealed with silicon grease. The volume of air around the specimen was reduced by enclosing the direct shear box and the assembly inside an airtight polythene bag which was then covered with a damp cloth to reduce any variations in temperature inside the polythene bag (Fig. 7). The moisture contents of soil specimens before the compaction and after the direct shear test were determined. However, the average moisture content variation was found to be negligible (< 0.1%). Therefore, soil specimen was assumed to be at a constant water content condition during compaction and shearing.

During the compression stage, the specimens were loaded vertically in 10, 20 and 40 kPa steps, where each load increment was left for one to two days until the variations of vertical displacement became insignificant (<1%). The specimens were then sheared at a relatively low shear strain rate of 0.006 mm/min, in order to accommodate the redistribution of any variation in matric suction induced by the shearing process. Shearing continued until a maximum shear strain of 25% was achieved.

## RESULTS AND DISCUSSION

### Stress-strain behaviour

The shear stress and strains of 147 soil samples were measured at three different normal loads for given osmotic suctions and various initial matric suctions. Of those, the distributions of shear stress and normal strain were plotted against the shear strain for different osmotic suctions for fully saturated conditions. The stress-strain behaviour of the fully saturated soil without the influence of salinity ($\pi$ = 0 kPa), was determined to consider as a reference to compare the stress-strain behaviour of the soil with variable osmotic suctions under unsaturated conditions.

The saturated stress-strain behaviour of the soil for various osmotic suctions for a given normal stress ($\sigma'_N$ = 10 kPa) is shown in Fig. 8. The results show that the peak shear stress increases gradually with the influence of osmotic suction, showing a maximum increase of around 13.48 kPa. Moreover, the stress-strain behaviour of the unsaturated soil was monitored for six different matric suction conditions as discussed above. Of those, the stress-strain distribution for two different pressure conditions (different applied normal stresses and matric suctions) is shown in Fig. 9. Similar to the behaviour of saturated soil, the peak stress of unsaturated soil increases with osmotic suction. The reason for this is the increased resistance for the relative movement of soil particles due to the increase in inter-particle bond strength. However, the increase of peak shear stress of unsaturated soil with respect to osmotic suction was higher compared to the saturated condition for a given normal stress. For example, the soil specimen subjected to 1500 kPa matric suction shows an increase of around 98.96 kPa of peak shear stress for the highest osmotic suction increase, while the saturated soil shows only about 13.48 kPa for the same increase of osmotic suction.

Hence, it is evident that both matric suction (as expected) and osmotic suction has a significant influence on the peak shear stress.

The influence of osmotic suction on normal strain response of the saturated and unsaturated soil for a given normal stress is shown in Fig. 8 and 9. The results indicate that for all the osmotic and matric suction conditions, the normal strain decreases, showing a contractive behaviour of the specimens. Furthermore, an increase in osmotic suction results in lower contraction of the specimen for both saturated and unsaturated conditions. Also, as expected, at higher matric suctions the specimens exhibit a lower contraction behaviour compared to saturated conditions. This contractive behaviour of soil specimens can be further elaborated with maximum normal strain results. The maximum normal strain is considered as the lowest achieved normal strain of the specimen. The distribution of maximum normal strain with respect to osmotic suction for various matric suctions for a given normal stress ($\sigma'_N$ = 10 kPa) is shown in Fig. 10. For all the matric suction conditions, the maximum normal strain significantly decreases with osmotic suction, showing the highest decrease of change of maximum normal strain of around 4.7%. This could be because of the increased resistance to the relative movement of particles due to the influence of osmotic suction. Further as expected, the change of maximum normal strain also decreases with matric suction. Interestingly, while the change of maximum normal strain without the influence of osmotic suction is around 2.7% ($\sigma'_N$ = 10 kPa), at higher matric suctions (1500 kPa) the change of maximum normal strain decreases to 0.27% for the same increase of osmotic suction.

**Model calibration and validation**

The peak shear strength was determined from the results of the direct shear tests. The summary of all the peak stress results is given in Table 2. The experimental distribution of $\chi_2$was calculated based on Equation (5). The saturated friction angle was calculated when the soil sample became fully saturated with distilled water ($\pi$ = 0 kPa). The unsaturated behaviour of soil is influenced by the level of matric suction. Therefore, the influence that the matric suction has on $\chi_2$was considered by incorporating the corresponding degree of saturation into Equation (6). Due to the limited available literature for this soil suction range, three independent data sets have been used for calibration (i.e. $\sigma'_N$ = 20 kPa) and validation (i.e. $\sigma'_N$ = 10 and 40 kPa). The proposed new model for $\chi_2$ [Equation(6)] was calibrated for three major initial matric suction conditions such as $s_i$ = 0 kPa (saturated), $s_i$ = 200 kPaand 500 kPa, with respect to experimental results for a given normal stress ($\sigma'_N$ = 20 kPa).The distribution of $\chi_2$ with the electrical conductivity ratio for three different levels of matric suctions is shown in Fig. 11; it was used to estimate the best-fit parameters which were then used to predict the unsaturated behaviour of soil in combination with the degree of saturation for the other independent data sets. The fully saturated condition was used to determinethe*a* and *b* coefficients when the influence of *c*was not significant ($S_r$ = 1). Then the parameter *c* was determined based on the results from $s_i$ = 200 kPa condition, and also further calibrated all the three parameters with $s_i$ = 500 kPa. Based on these determinations, the calibrated parameters are *a* = 0.003, *b* = 0.0375 and *c* = 2. The proposed model was validated for two independent loading conditions ($\sigma'_N$ = 10 and 40 kPa) with the calibrated model parameters, and the corresponding validation results are shown in Fig. 12. In general, the model predictions match the experimental results very well, thus indicating that the proposed model incorporating$\chi_2$is able topredictthe osmotically induced shear strength of a saline soil.

The above results also show that $\chi_2$ increases with an increasing ECR ($\Delta EC/EC_i$), but this increase in $\chi_2$ also decreased at high ECR values until it reached a maximum theoretical $\chi_2$ value of 0.003 under saturated conditions irrespective of applied stress. The maximum theoretical $\chi_2$ increases as the initial degree of saturation decreases or the initial matric suction increases. The minimum value of ECR where $\chi_2$ reached its maximum or the critical ECR ($ECR_c$), does not depend on the initial matric suction; hence it is evident that the $ECR_c$ is a parameter which only depends on the pore solution and surface potential of soil particles.

The predicted peak shear stress was calculated based on Equation (3) and the results were compared with the experimental results for two independent applied normal stress conditions; the corresponding distribution of model prediction and experimental results of peak shear stress is shown in Fig. 13.The model predictions match the experimental results at lower initial matric suctions (< 500 kPa), giving a maximum deviation of less than 5kPa. However, as the initial matric suction (>500 kPa) increases, the model shows a slight deviation (5 to 14.5 kPa) depending on the magnitude of osmotic suction and matric suction. Overall, the model exhibits an increased deviation from the experimental results at the highest values of osmotic suction and initial matric suction. The maximum deviation of model results from experimental results for any condition is about 14.5kPa when the osmotic suction increases to 9560 kPa at the highest considered initial matric suction of 1500 kPa.

## MODEL LIMITATIONS

The proposed unsaturated shear strength model was primarily based on the salinity level (hence, osmotic suction) and the initial matric suction. The model was calibrated and validated using the shear box results for a clayey soil of low plasticity (CL; PI=19) under constant water content. The measured maximum matric suction changes upon shearing were generally very small compared to the relatively high initial matric suction, as shown in Fig. 14 for a typical test specimen. Therefore, while the proposed model is accurate under these specific conditions, when considering its broader application to other soils, the following limitations can be elucidated.

- This unsaturated shear strength model was validated only for a single soil of low plasticity (CL). Therefore, the application of the model to soils of much higher plasticity(e.g. CH, OH, MH) will require caution to be exercised.
- Duringshearing (constant water content) the pore structure (void ratio) can change with an accompanied change in the degree of saturation. Fig. 14 shows for an initial matric suction of 1500 kPa, the maximum change in matric suction upon shearing is in the proximity of 35 kPa (< 2.5%). For soils of different fabric that significantly dilate upon shearing(e.g. dense granular soils or highly compacted fills), the shearing-induced matric suction changes may be large enough to induce notable discrepancies of the proposed shear strength model.
- Under near saturation, the role of matric suction will be eliminated, hence the shear strength parameter ($\chi_2$) represented by Equation (6)becomes simplified as a sole function ofsalinity. In this regard, further tests conducted at much greater osmotic suction (e.g. in the proximity of say 100 MPa)will be desirable to calibrate$\chi_2$more accurately.
- It is appreciated that remoulded soil specimens may not truly represent the actual hydro-mechanical behaviour of in situ soil. However, due to technical difficulties in obtaining many identical undisturbed test specimens (i.e. same microstructure and pore water salinity), remoulded samples were used for this study.Undisturbed block

samples to fit the dimensions of the shear box apparatus will certainly be considered in the future.

- In the field, given the climatic and environmental influences, the pore water salinity can vary with time due to ion exchange. In this study, time-dependent change in salinity was not considered.
- The proposed model was influenced by electrical conductivity measurement, where only the role of NaCl was considered. However, the model can deviate from accuracy if the soil solution containsother cations such as $Fe^{3+}$ or $Fe^{2+}$.
- At very high matric suctions existing under exceedingly dry conditions, the effect ofsalt crystallisation on the soil shear strength cannot be predicted by this model.

## CONCLUSION

A series of direct shear box tests were carried out on a typical unsaturated saline soil (CL) subjected to different levels of osmotic suction with known values of initial matric suction. While still embracing the Mohr-Coulomb mathematical framework, this study proposed a new relationship to capture the role of osmotic suction by introducing a newparameter $\chi_2$(i.e. as an independent term to$\chi_1$) in the original Bishop's unsaturated shear strength model modified by Khabbaz and Khalili (1998). The following key conclusions can be drawn based on the results of this study.

- The parameter $\chi_2$representing the role of osmoticcomponent can be estimated based on the electrical conductivity ratio (ECR).The maximum value of $\chi_2$and the corresponding minimum (critical)value $ECR_c$for a given degree of saturation define the appropriate bounds of $\chi_2$ that reaches its maximum of 0.003 when $ECR_c$ = 900 at full-saturation ($S_r$= 1).

- At lower values of both osmotic suction and initial matric suction, the predicted value of $\chi_2$from Equation (6) agrees with the experimental resultsfor $a$ = 0.003, $b$ = 0.0375 and $c$ = 2. However, at high levels of osmotic suction(i.e. $\pi$ > 4500 kPa)and at high initial matric suction(i.e. $s_i$> 500 kPa), the model deviates from accuracy.
- The results of this study prove that for a given increase in osmotic suction, the peak shear stress can significantly increase for both the unsaturated and saturated soil specimens. For the unsaturated soil subjected to an initial matric suction of 1500 kPa, when the osmotic suction increased from 0 to 9560 kPa, the corresponding peak shear stress increased significantly by about 75% from 133 kPa to 232 kPa. For the same increase in osmotic suction, the corresponding increase in peak shear stress of saturated test specimens from 11.5 kPa to 24.9 kPa may not seem substantial at a glance, but it is noteworthy that this increase is still more than double, hence demonstrating the beneficial influence of salinity even under saturated conditions.

## DATA AVAILABILITY STATEMENT

All data, models, and code generated or used during the study appear in the submitted article.

## ACKNOWLEDGMENT

The authors wish to acknowledge the financial support provided by the Australian Government Research Training Program Scholarship and ARC Industry Transformation Training Centre for Advanced Rail Track Technologies (ITTC-Rail). The authors also appreciate the assistance provided by the University of Wollongong (UOW) technical staff member, Richard Berndt. The authors also acknowledge the contributions of past PhD students and Research associates at UOW who have conducted research on native vegetationand unsaturated soil mechanics, namely Dr BehzadFatahi, Dr ShiranGunasena, Dr UdeshiniPathirage and Dr MudithaPallewatha.

REFERENCES

ABEDI-KOUPAI, J. & MEHDIZADEH, H. 2007. Estimation of osmotic suction from electrical conductivity and water content measurements in unsaturated soils. *Geotechnical Testing Journal,* 31**,** 142-148.

ADAM, I., MICHOT, D., GUERO, Y., SOUBEGA, B., MOUSSA, I., DUTIN, G. & WALTER, C. 2012. Detecting soil salinity changes in irrigated Vertisols by electrical resistivity prospection during a desalinisation experiment. *Agricultural water management,* 109**,** 1-10.

ARORA, S. 2017. Diagnostic properties and constraints of salt-affected soils. *Bioremediation of Salt Affected Soils: An Indian Perspective.* Springer.

BARBOUR, S. & FREDLUND, D. 1989. Mechanisms of osmotic flow and volume change in clay soils. *Canadian Geotechnical Journal,* 26**,** 551-562.

BISHOP, A. W. 1960. The principles of effective stress, *Norges Geotekniske Institute*.

DI MAIO, C., SANTOLI, L. & SCHIAVONE, P. 2004. Volume change behaviour of clays: the influence of mineral composition, pore fluid composition and stress state. *Mechanics of materials,* 36**,** 435-451.

DI MAIO, C. & SCARINGI, G. 2016. Shear displacements induced by decrease in pore solution concentration on a pre-existing slip surface. *Engineering geology,* 200**,** 1-9.

FREDLUND, D. G., RAHARDJO, H. & FREDLUND, M. D. 2012. Unsaturated soil mechanics in engineering practice, *John Wiley & Sons*.

GALLAGE AND UCHIMURA 2015. Direct Shear Testing on Unsaturated Silty Soils to Investigate the Effects of Drying and Wetting on Shear Strength Parameters at Low Suction *Journal of Geotechnical and Geoenvironmental Engineering*, Vol. 142, Issue 3 (March 2016).

GARAKANI, A.A., HAERI, S.M., CHERATI, D.Y., GIVI, F.A., TADI, M.K., HASHEMI, A.H., CHITI, N. AND QAHREMANI, F., 2018. Effect of road salts on the hydro-mechanical behavior of unsaturated collapsible soils. *Transportation Geotechnics*, 17, pp.77-90.

GRAHAM, J., OSWELL, J. & GRAY, M. 1992. The effective stress concept in saturated sand-clay buffer. *Canadian Geotechnical Journal,* 29**,** 1033-1043.

HEN-JONES, R., HUGHES, P., GLENDINNING, S., GUNN, D., CHAMBERS, J., WILKINSON, P. & UHLEMANN, S. 2014. Determination of moisture content and soil suction in engineered fills using electrical resistivity. *CRC Press/Balkema*.

JAYATHILAKA, P., INDRARATNA, B. & HEITOR, A. 2019. Influence that Osmotic Suction and Tree Roots has on the Stability of Coastal Soils. *Geotechnics for Transportation Infrastructure.* Springer.

JIAO-JUN, Z., HONG-ZHANG, K. & GONDA, Y. 2007. Application of Wenner configuration to estimate soil water content in pine plantations on sandy land. *Pedosphere,* 17**,** 801-812.

JOTISANKASA A., MAIRAING W., 2010. “Suction-monitored direct shear testing of residual soils from landslide-prone areas”, *Journal of Geotechnical and Geoenvironmental Engineering*, Vol. 136, No. 3: p. 533-537.

KHABBAZ, M. & KHALILI, N. 1998. A unique relationship for chi for the determination of the shear strength of unsaturated soils. *Geotechnique,* 48**,** 681-687.

KHALILI, N. 2018. Guidelines for the application of effective stress principle to shear strength and volume change determination in unsaturated soils. *Australian Geomechanics Journal,* 53**,** 37-47.

KHALILI, N., GEISER, F. & BLIGHT, G. 2004. Effective stress in unsaturated soils: Review with new evidence. *International journal of Geomechanics,* 4**,** 115-126.

LI, S., LI, H., XU, C.-Y., HUANG, X.-R., XIE, D.-T. & NI, J.-P. 2013. Particle interaction forces induce soil particle transport during rainfall. *Soil Science Society of America Journal,* 77**,** 1563-1571.

LIANG, Y., HILAL, N., LANGSTON, P. & STAROV, V. 2007. Interaction forces between colloidal particles in liquid: Theory and experiment. *Advances in colloid and interface science,* 134**,** 151-166.

LU, N. & LIKOS, W. J. 2006. Suction stress characteristic curve for unsaturated soil. *Journal of geotechnical and geoenvironmental engineering,* 132**,** 131-142.

MURRAY, E. J. & SIVAKUMAR, V. 2010. Unsaturated soils: a fundamental interpretation of soil behaviour, *John Wiley & Sons*.

PATHIRAGE, U., INDRARATNA, B., PALLEWATTHA, M. & HEITOR, A. 2017. A theoretical model for total suction effects by tree roots. *Environmental Geotechnics*, 1-8.

PIEGARI, E. & MAIO, R. D. 2013. Estimating soil suction from electrical resistivity. *Natural Hazards and Earth System Sciences,* 13, 2369-2379.

RAO, S. M. & THYAGARAJ, T. 2007. Swell–compression behaviour of compacted clays under chemical gradients. *Canadian geotechnical journal,* 44, 520-532.

READ, D. & CAMERON, D. 1979. Relationship between salinity and Wenner resistivity for some dryland soils. *Canadian Journal of Soil Science,* 59, 381-385.

RENGASAMY, P. 2006. World salinization with emphasis on Australia. *Journal of experimental botany,* 57, 1017-1023.

SHAH, P. H. & SINGH, D. 2004. A simple methodology for determining electrical conductivity of soils. *Journal of ASTM International,* 1, 1-11.

SHEVNIN, V., PEINADO, H., DELGADO, O. & RYJOV, A. Petrophysical and Electrical Study of Soil Properties in Sinaloa, Mexico. Near Surface 2010-16th EAGE European Meeting of Environmental and Engineering Geophysics, 2010.

TARANTINO A., TOMBOLATO S., 2005. "Coupling of hydraulic and mechanical behaviour in unsaturated compacted clay", *Geotechnique* 55 (4): p. 307–317.

TIWARI, B. & AJMERA, B. 2014. Reduction in fully softened shear strength of natural clays with NaCl leaching and its effect on slope stability. *Journal of Geotechnical and Geoenvironmental Engineering,* 141, 04014086.

VAN GENUCHTEN, M. T. 1980. A closed-form equation for predicting the hydraulic conductivity of unsaturated soils. *Soil science society of America journal,* 44**,** 892-898.

VANAPALLI, S., FREDLUND, D., PUFAHL, D. & CLIFTON, A. 1996. Model for the prediction of shear strength with respect to soil suction. *Canadian Geotechnical Journal*, 33, 379-392.

XU, Y. 2019. Peak shear strength of compacted GMZ bentonites in saline solution. *Engineering Geology,* 251**,** 93-99.

LIST OF TABLES

Table 1The osmotic suctions at different concentrations of NaCl

| **Concentration (mol/L)** | **Measured osmotic suction (kPa)** |
|---|---|
| 0.0 | 0.0 |
| 0.2 | 910 |
| 0.4 | 1790 |
| 0.6 | 2700 |
| 0.8 | 3690 |
| 1.0 | 4650 |
| 2.0 | 9560 |

Table 2 Experimental summary of peak shear stress

| Matric suction (kPa) | $\sigma'_N$ (kPa) | Peak shear stress (kPa) | | | | | | |
|---|---|---|---|---|---|---|---|---|
| | | $\pi$ = 0 kPa | $\pi$ = 910 kPa | $\pi$ = 1790 kPa | $\pi$ = 2700 kPa | $\pi$ = 3690 kPa | $\pi$ = 4650 kPa | $\pi$ = 9560 kPa |
| 0 | 10 | 11.46 | 11.71 | 12.71 | 13.96 | 15.48 | 17.02 | 24.93 |
| | 20 | 16.49 | 16.89 | 18.01 | 18.99 | 20.54 | 22.55 | 31.05 |
| | 40 | 27.29 | 27.69 | 28.54 | 29.79 | 31.09 | 33.79 | 42.56 |
| 25 | 10 | 24.62 | 24.97 | 26.12 | 27.42 | 29.32 | 30.92 | 37.99 |
| | 20 | 29.71 | 30.11 | 31.63 | 32.21 | 34.51 | 35.61 | 45.30 |
| | 40 | 40.45 | 40.83 | 41.93 | 42.85 | 44.95 | 46.58 | 56.30 |
| 100 | 10 | 47.42 | 47.71 | 49.11 | 51.29 | 53.64 | 55.81 | 65.47 |
| | 20 | 52.30 | 52.89 | 54.30 | 55.96 | 58.74 | 60.05 | 74.51 |
| | 40 | 63.24 | 63.60 | 65.43 | 66.95 | 68.69 | 71.99 | 83.35 |
| 200 | 10 | 60.58 | 61.33 | 63.26 | 65.70 | 68.39 | 71.92 | 84.98 |
| | 20 | 65.89 | 66.41 | 68.72 | 71.25 | 73.14 | 77.66 | 93.11 |
| | 40 | 76.32 | 76.90 | 79.43 | 80.89 | 83.18 | 87.87 | 103.43 |
| 500 | 10 | 85.65 | 86.54 | 90.97 | 94.95 | 100.09 | 105.88 | 129.04 |
| | 20 | 90.75 | 92.17 | 94.30 | 99.62 | 105.63 | 110.97 | 137.16 |
| | 40 | 101.46 | 102.63 | 106.04 | 108.99 | 113.91 | 120.57 | 149.33 |
| 1000 | 10 | 112.81 | 114.37 | 120.08 | 127.35 | 135.70 | 142.78 | 187.60 |
| | 20 | 118.00 | 120.08 | 125.66 | 130.99 | 142.94 | 149.74 | 196.51 |
| | 40 | 128.58 | 130.14 | 136.37 | 145.20 | 150.44 | 160.21 | 204.57 |
| 1500 | 10 | 133.10 | 135.47 | 143.55 | 152.41 | 162.42 | 173.77 | 232.05 |
| | 20 | 137.20 | 139.80 | 147.26 | 153.43 | 168.36 | 178.99 | 239.32 |
| | 40 | 148.90 | 150.65 | 158.51 | 167.73 | 182.01 | 190.48 | 245.12 |

LIST OF FIGURES

Fig. 12 Experimental and model prediction results of $\chi_2$ for different initial matric suctions with *a* = 0.003, *b* = 0.0375 and *c* = 2.0, when (a) $\sigma_N'$ = 10 kPa and (b) $\sigma_N'$ = 40 kPa

Fig.13 Distribution of experimental and model peak shear stress for different initial matric suctions and saturated osmotic suction, (a) $\sigma_N'$ = 10 kPa and (b) $\sigma_N'$ = 40 kPa

Fig. 14 Variation of matric suction during shearing ($\sigma_N'$ = 10 kPa and π = 0 kPa)

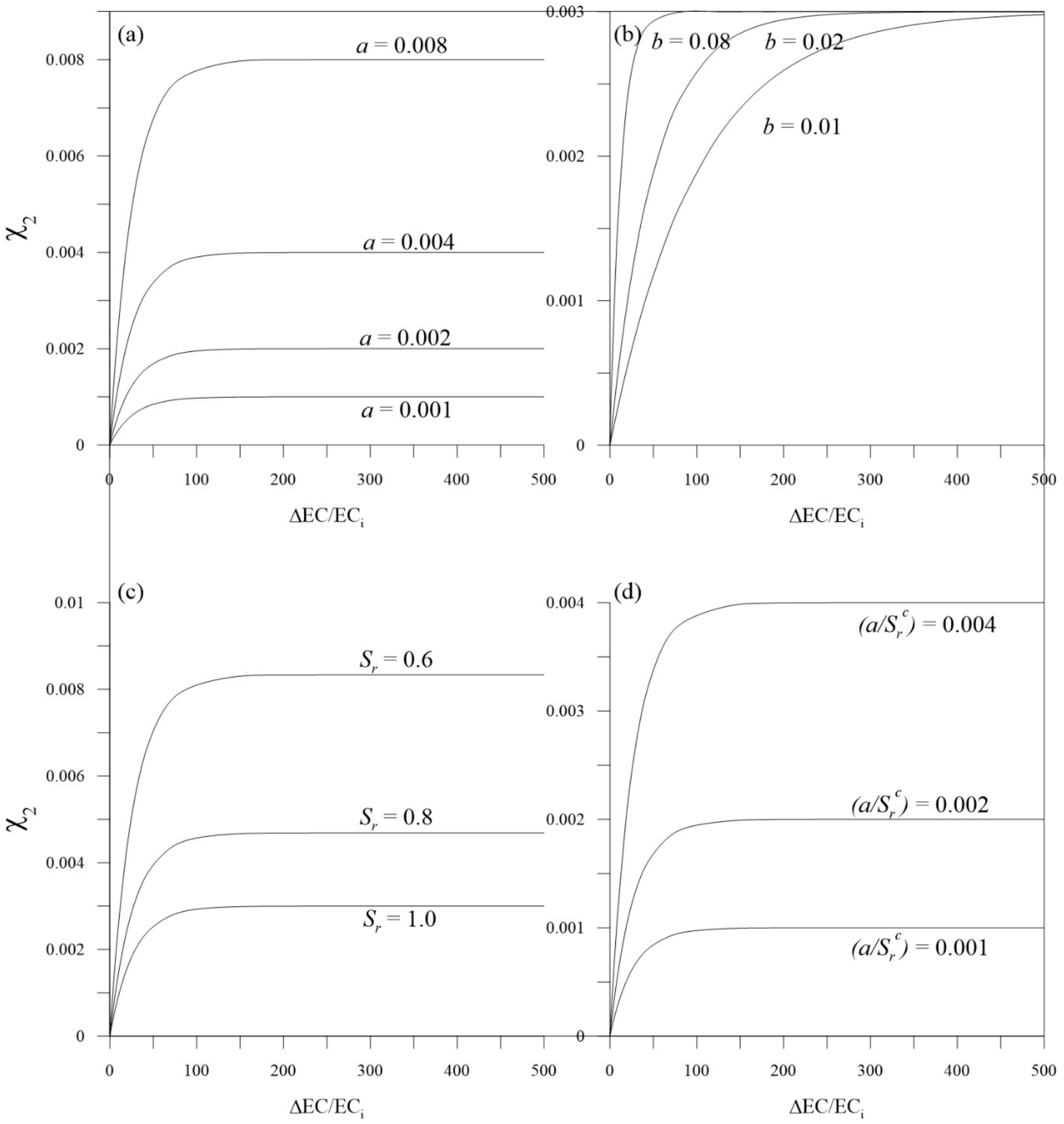
(a)
a = 0.008
a = 0.004
a = 0.002
a = 0.001
χ2
ΔEC/ECi
(b)
b = 0.08
b = 0.02
b = 0.01
ΔEC/ECi
(c)
Sr = 0.6
Sr = 0.8
Sr = 1.0
χ2
ΔEC/ECi
(d)
(a/Sr^c) = 0.004
(a/Sr^c) = 0.002
(a/Sr^c) = 0.001
ΔEC/ECi

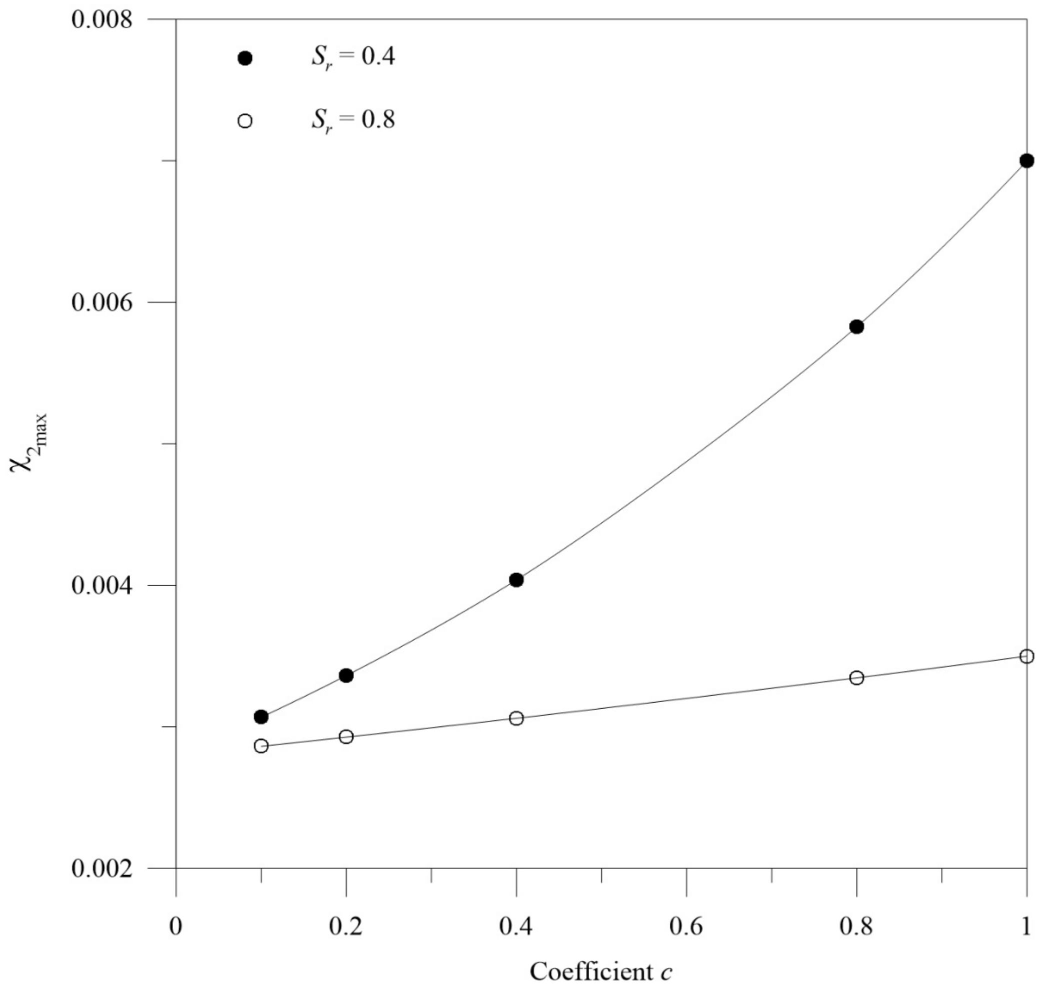

0.008
0.006
0.004
0.002
$\chi_{2_{\max}}$
$S_r$ = 0.4
$S_r$ = 0.8
0
0.2
0.4
0.6
0.8
1
Coefficient $c$

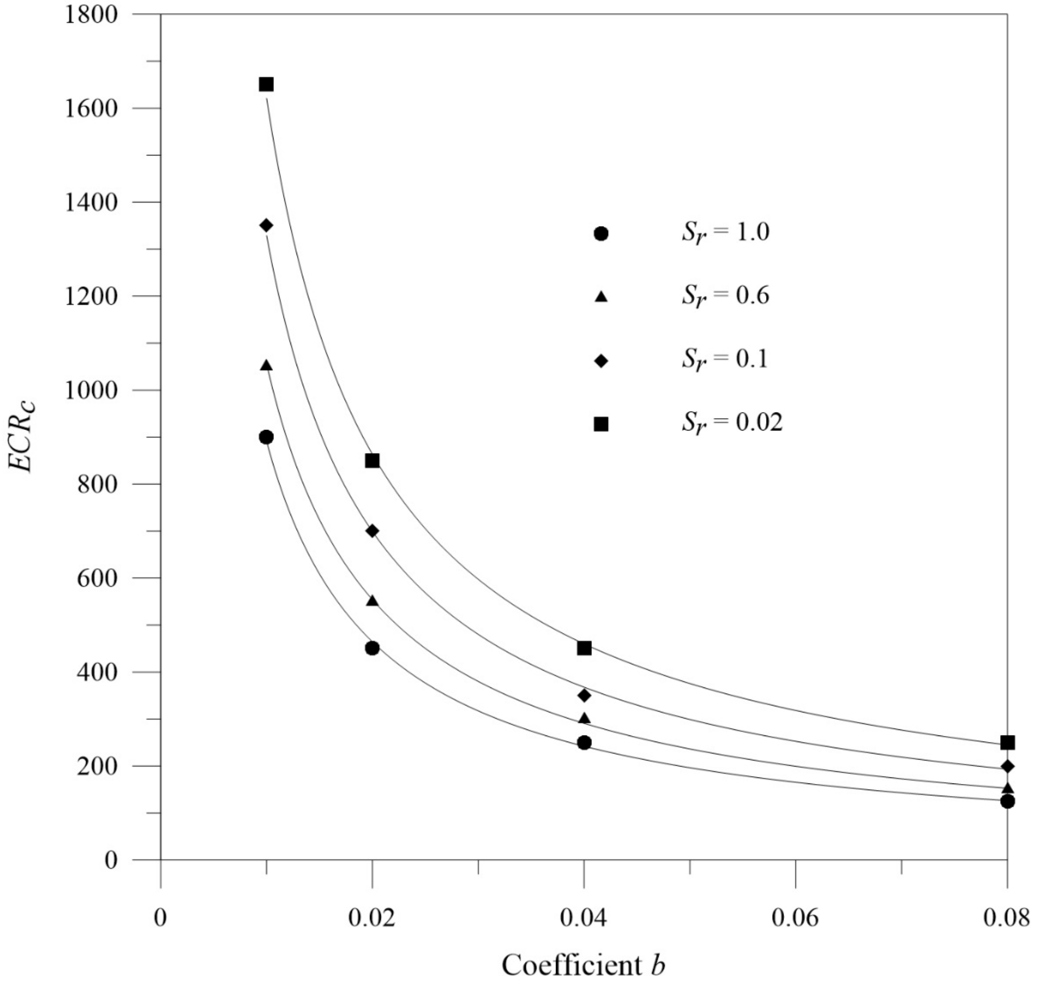
1800
1600
1400
1200
1000
800
600
400
200
0
0
0.02
0.04
0.06
0.08
Coefficient $b$
$ECR_c$
$S_r$ = 1.0
$S_r$ = 0.6
$S_r$ = 0.1
$S_r$ = 0.02

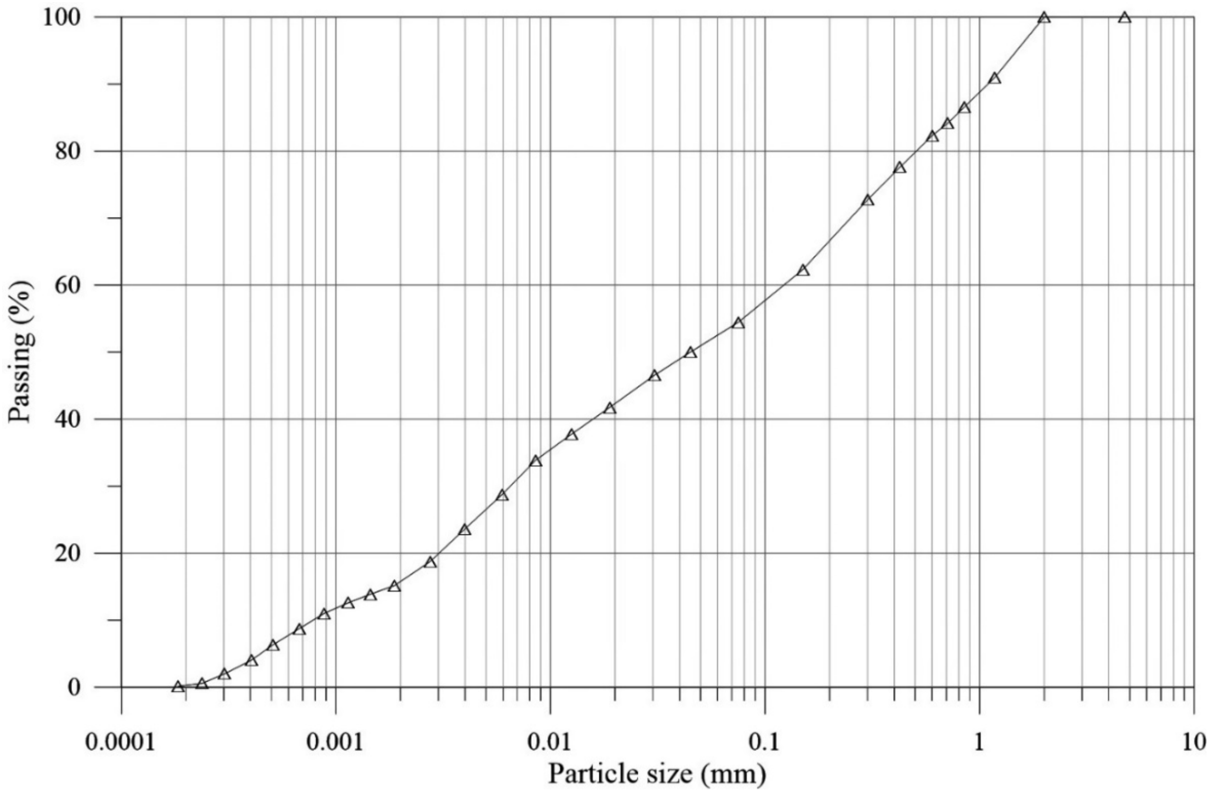
Passing (%)
0
20
40
60
80
100
0.0001
0.001
0.01
0.1
1
10
Particle size (mm)

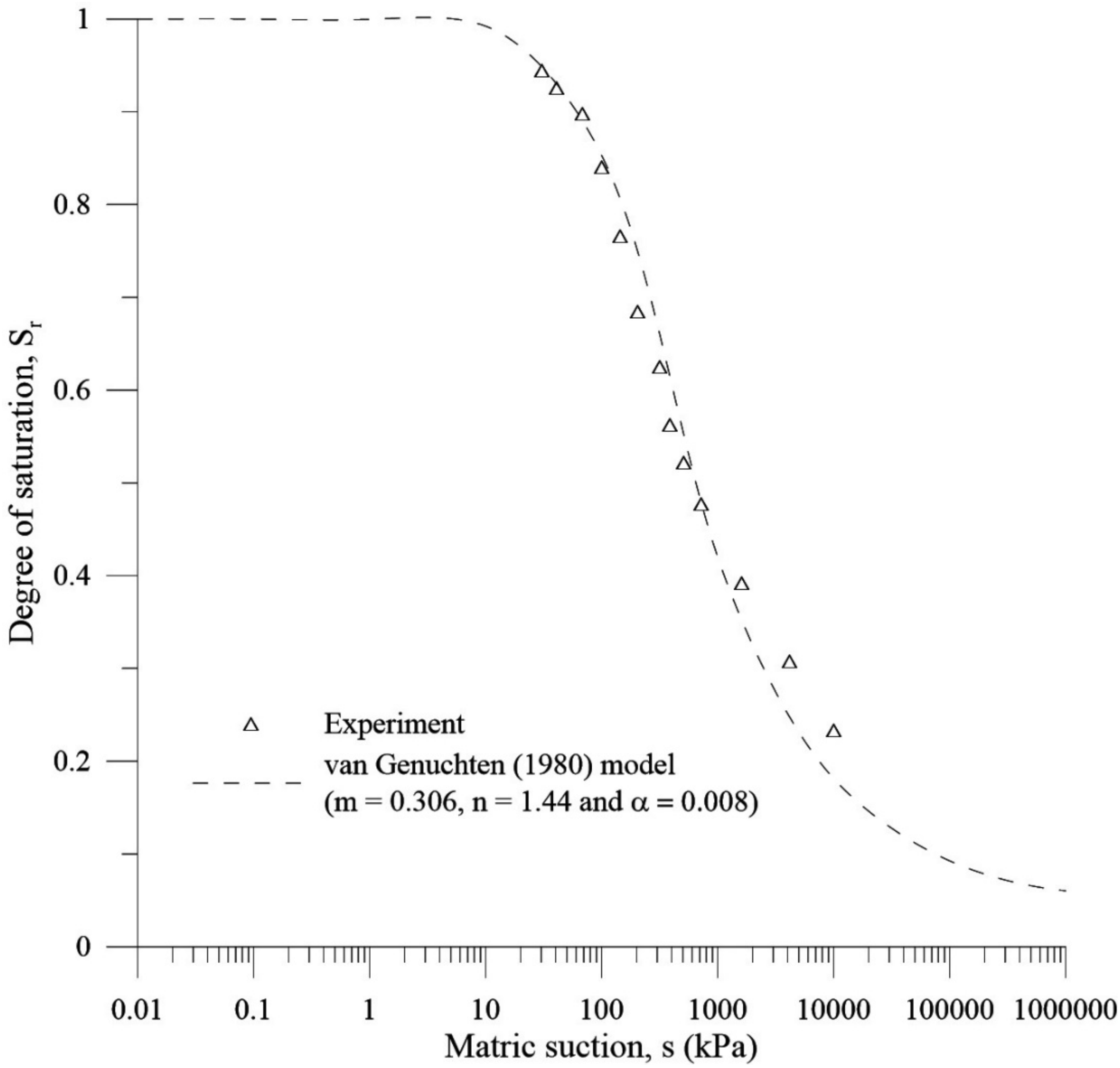
Degree of saturation, $S_r$
1
0.8
0.6
0.4
0.2
0
Experiment
van Genuchten (1980) model
(m = 0.306, n = 1.44 and α = 0.008)
0.01
0.1
1
10
100
1000
10000
100000
1000000
Matric suction, s (kPa)

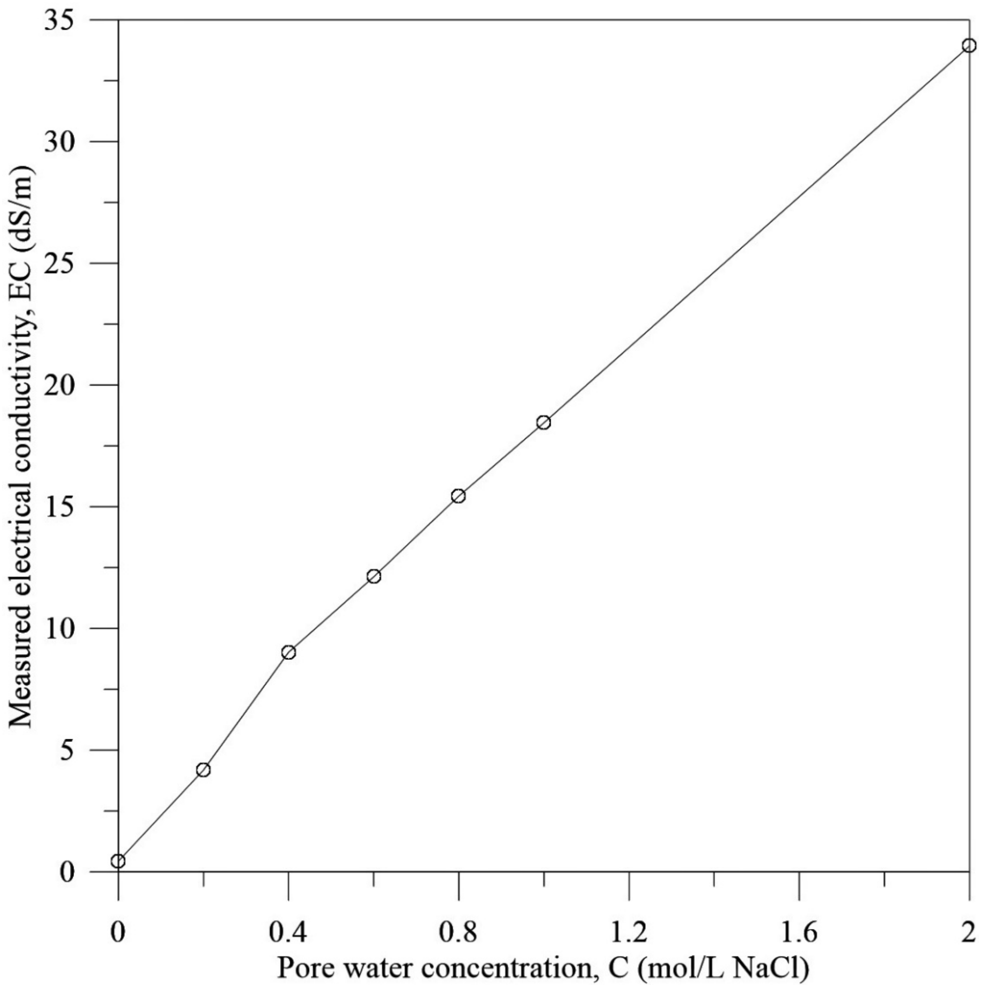
Measured electrical conductivity, EC (dS/m)
0
5
10
15
20
25
30
35
0
0.4
0.8
1.2
1.6
2
Pore water concentration, C (mol/L NaCl)

(a)

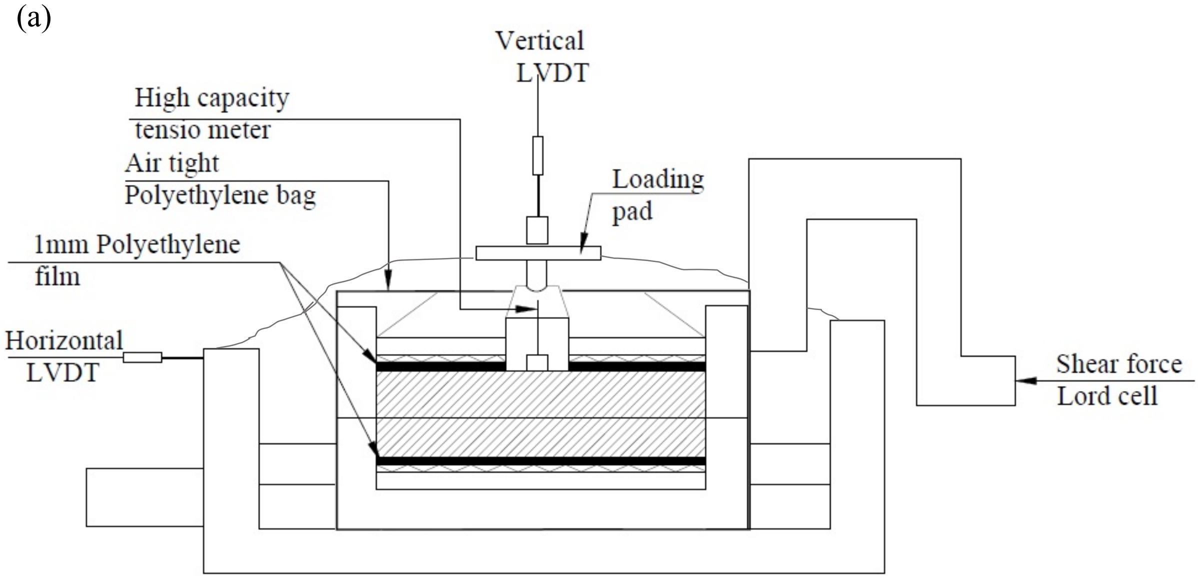
Vertical
LVDT
High capacity
tensio meter
Air tight
Polyethylene bag
Loading
pad
1mm Polyethylene
film
Horizontal
LVDT
Shear force
Lord cell

(b)

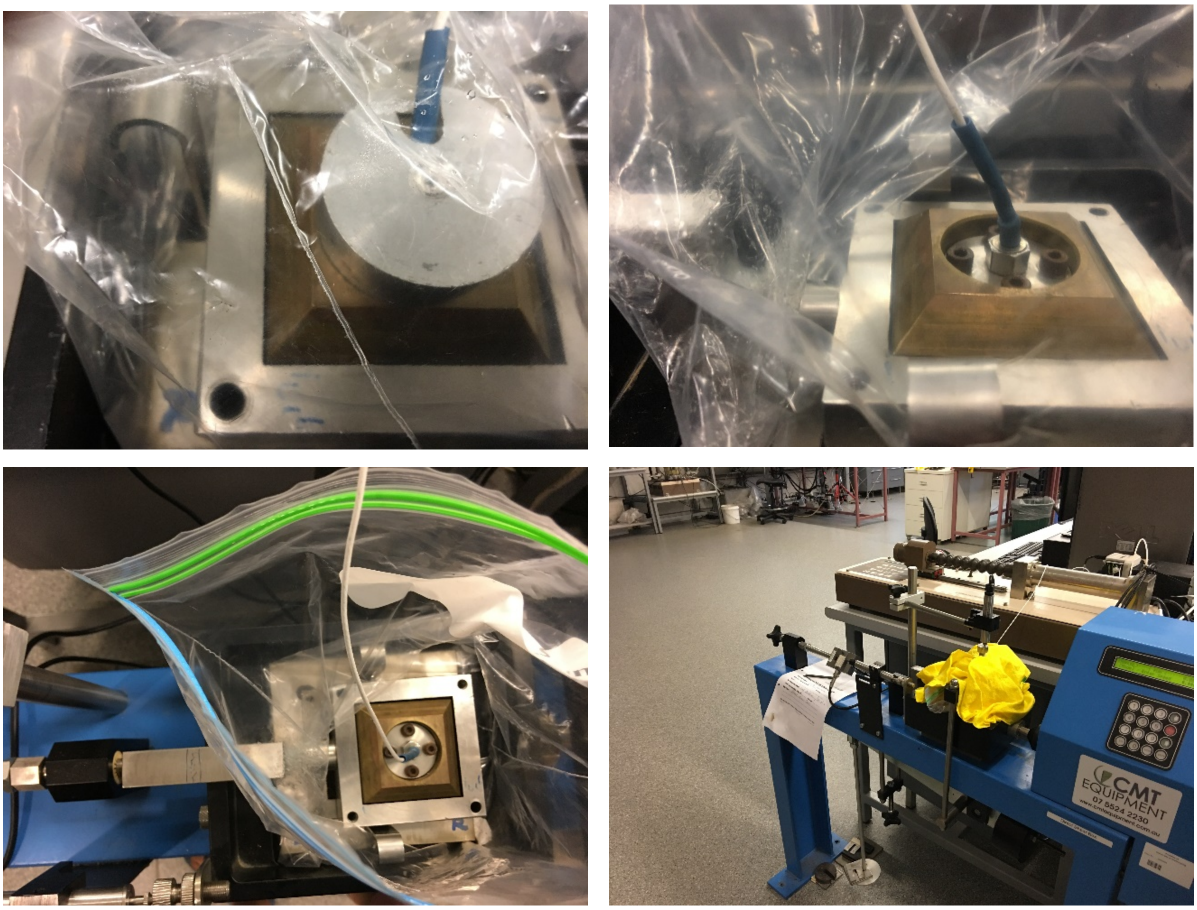
CMT
EQUIPMENT

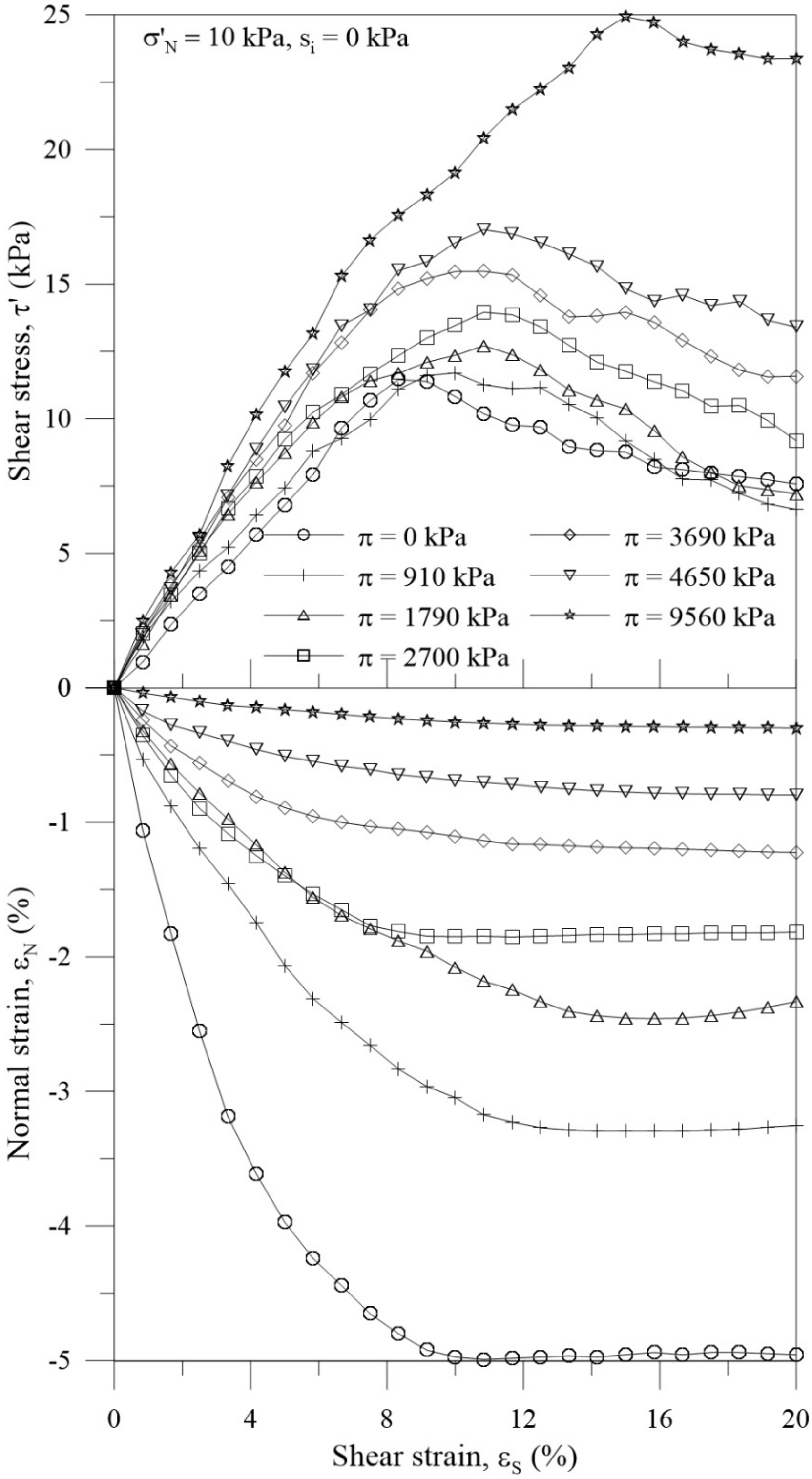
σ'N = 10 kPa, si = 0 kPa
Shear stress, τ' (kPa)
Normal strain, εN (%)
Shear strain, εS (%)
π = 0 kPa
π = 910 kPa
π = 1790 kPa
π = 2700 kPa
π = 3690 kPa
π = 4650 kPa
π = 9560 kPa
25
20
15
10
5
0
-1
-2
-3
-4
-5
0
4
8
12
16
20

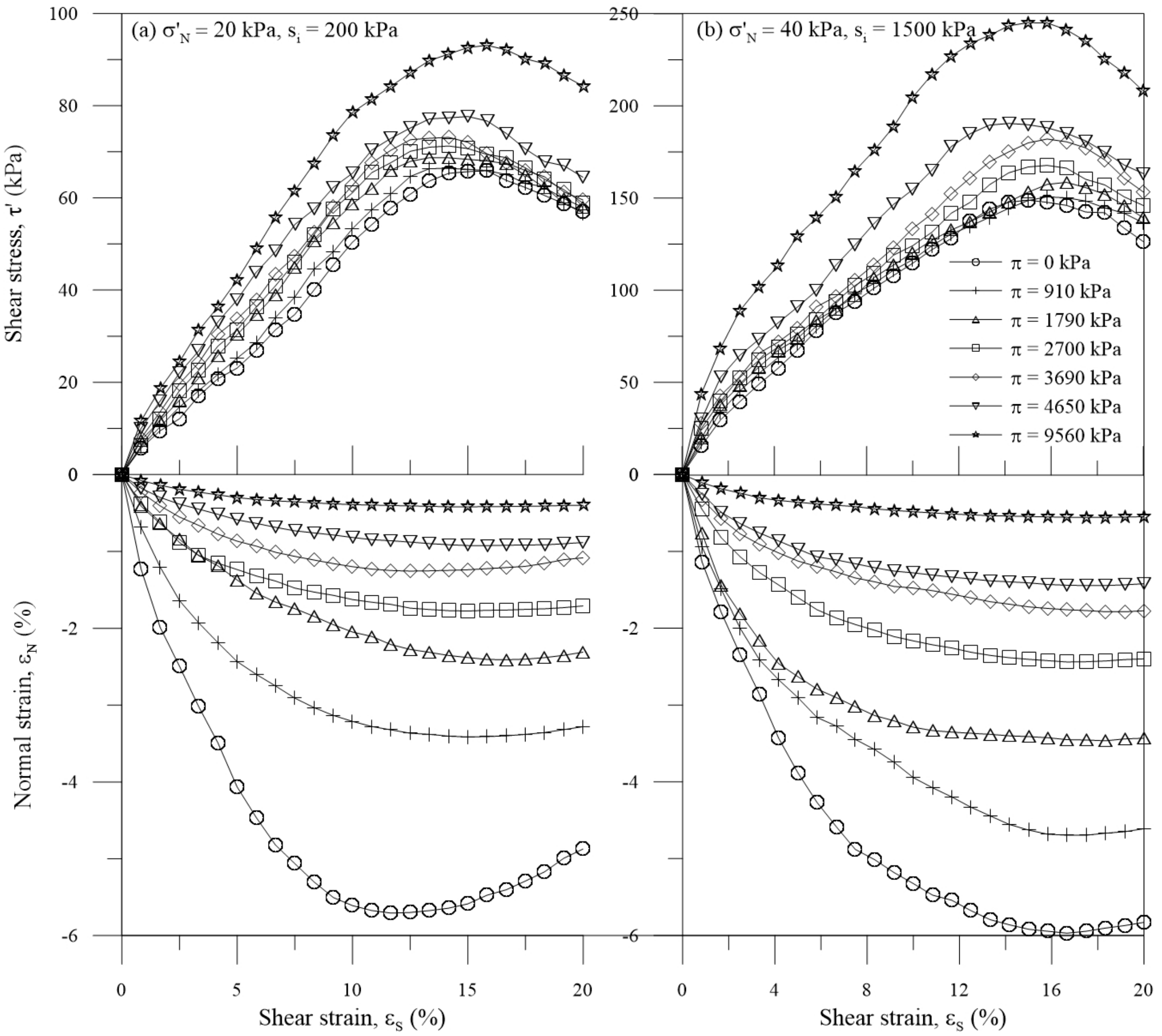
(a) σ'N = 20 kPa, si = 200 kPa
(b) σ'N = 40 kPa, si = 1500 kPa
Shear stress, τ' (kPa)
Normal strain, εN (%)
Shear strain, εS (%)
π = 0 kPa
π = 910 kPa
π = 1790 kPa
π = 2700 kPa
π = 3690 kPa
π = 4650 kPa
π = 9560 kPa

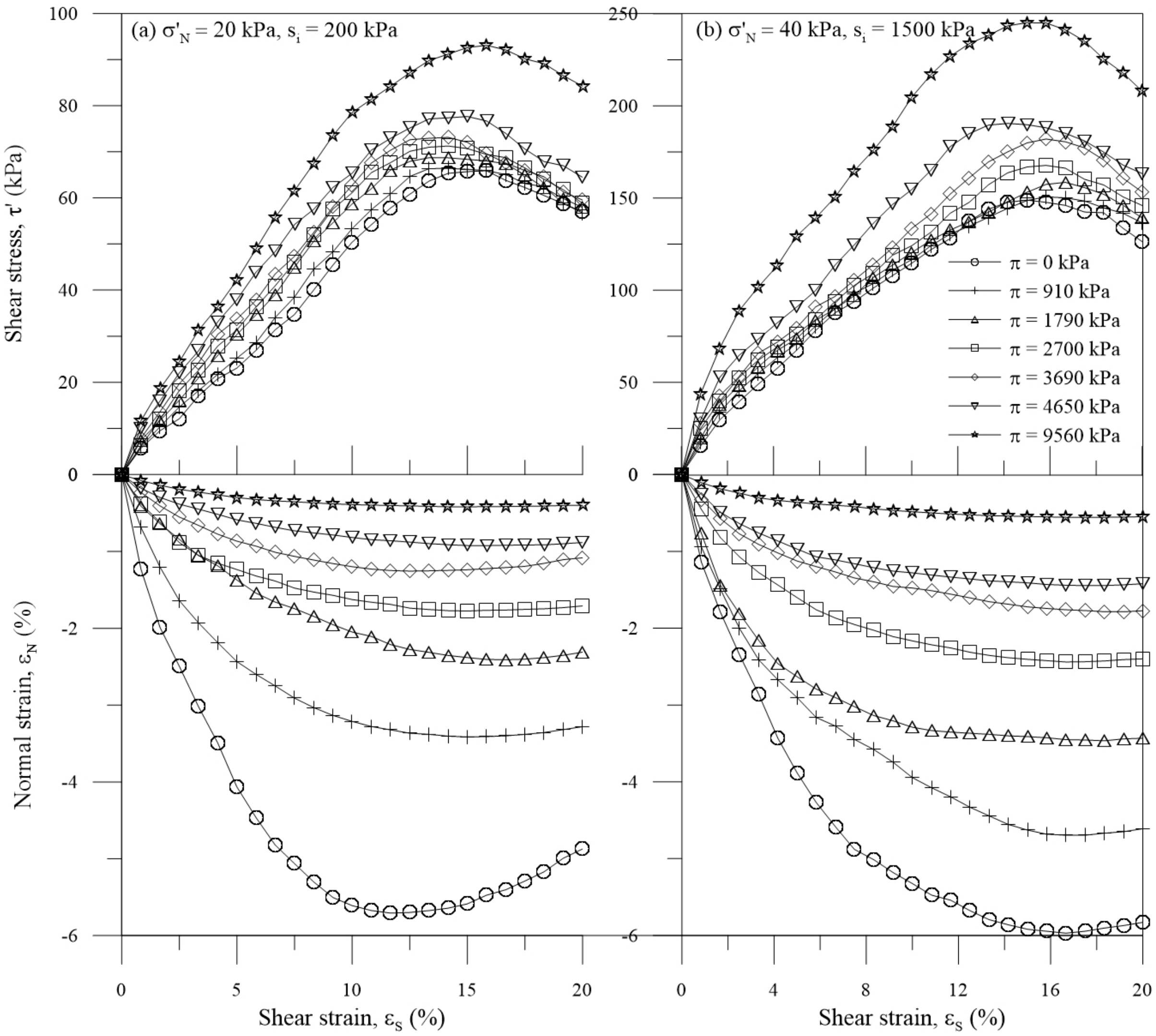
(a) σ'N = 20 kPa, si = 200 kPa
(b) σ'N = 40 kPa, si = 1500 kPa
Shear stress, τ' (kPa)
Normal strain, εN (%)
Shear strain, εS (%)
π = 0 kPa
π = 910 kPa
π = 1790 kPa
π = 2700 kPa
π = 3690 kPa
π = 4650 kPa
π = 9560 kPa

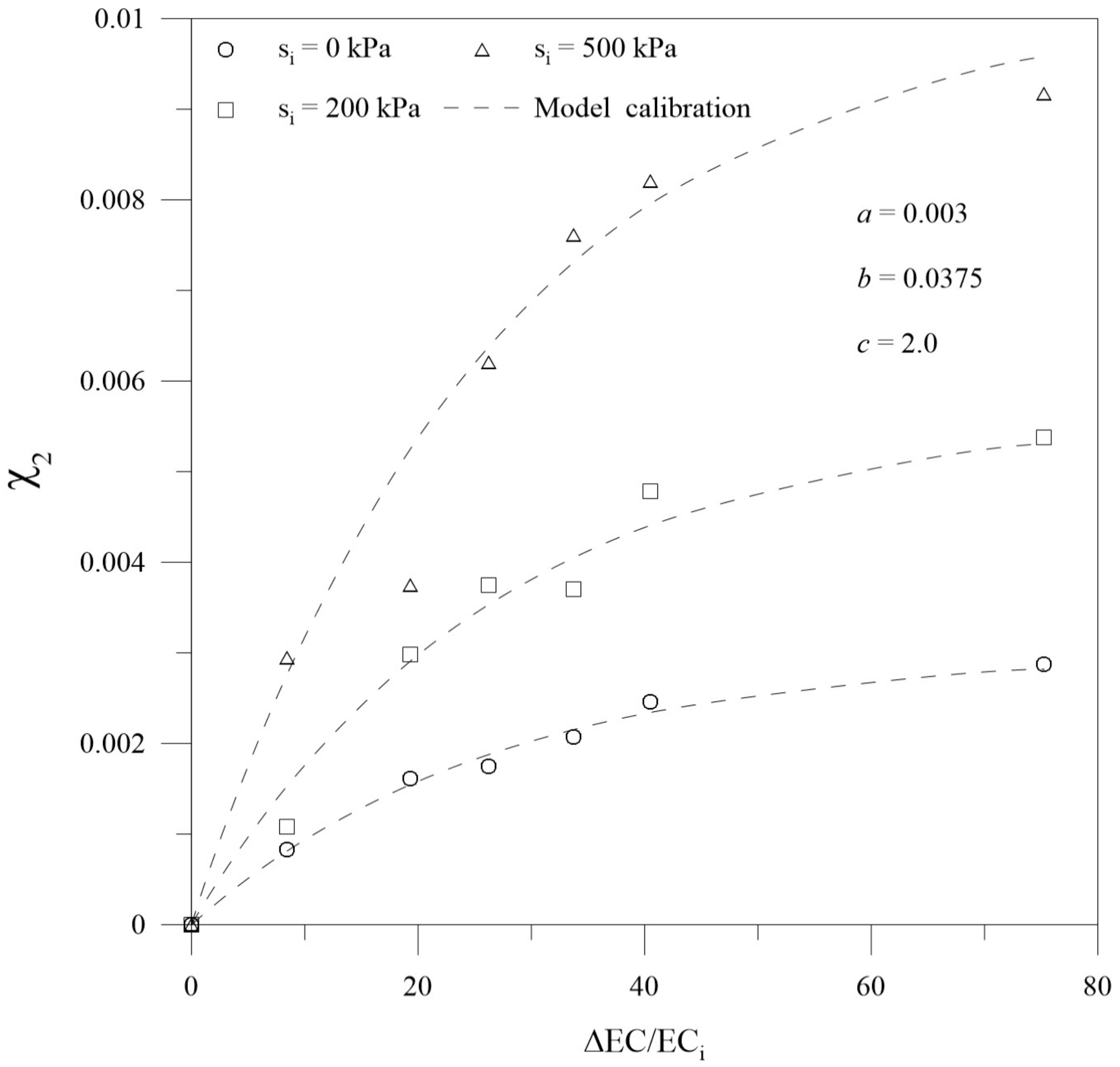

s_i = 0 kPa
s_i = 500 kPa
s_i = 200 kPa
Model calibration
a = 0.003
b = 0.0375
c = 2.0
χ2
ΔEC/ECi
0.01
0.008
0.006
0.004
0.002
0
20
40
60
80

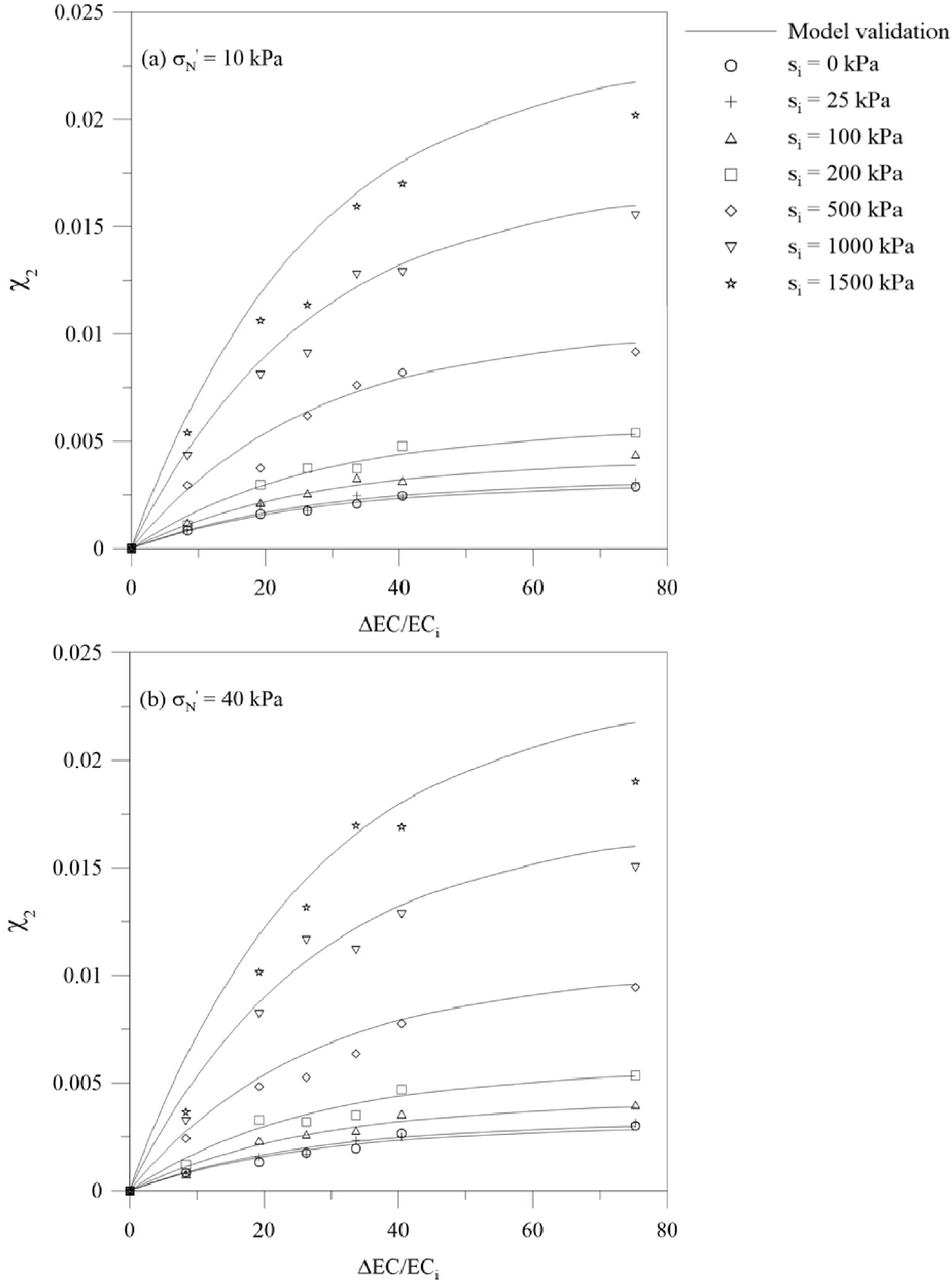
Model validation
si = 0 kPa
si = 25 kPa
si = 100 kPa
si = 200 kPa
si = 500 kPa
si = 1000 kPa
si = 1500 kPa
(a) σN' = 10 kPa
(b) σN' = 40 kPa
χ2
ΔEC/ECi
0.025
0.02
0.015
0.01
0.005
0
20
40
60
80

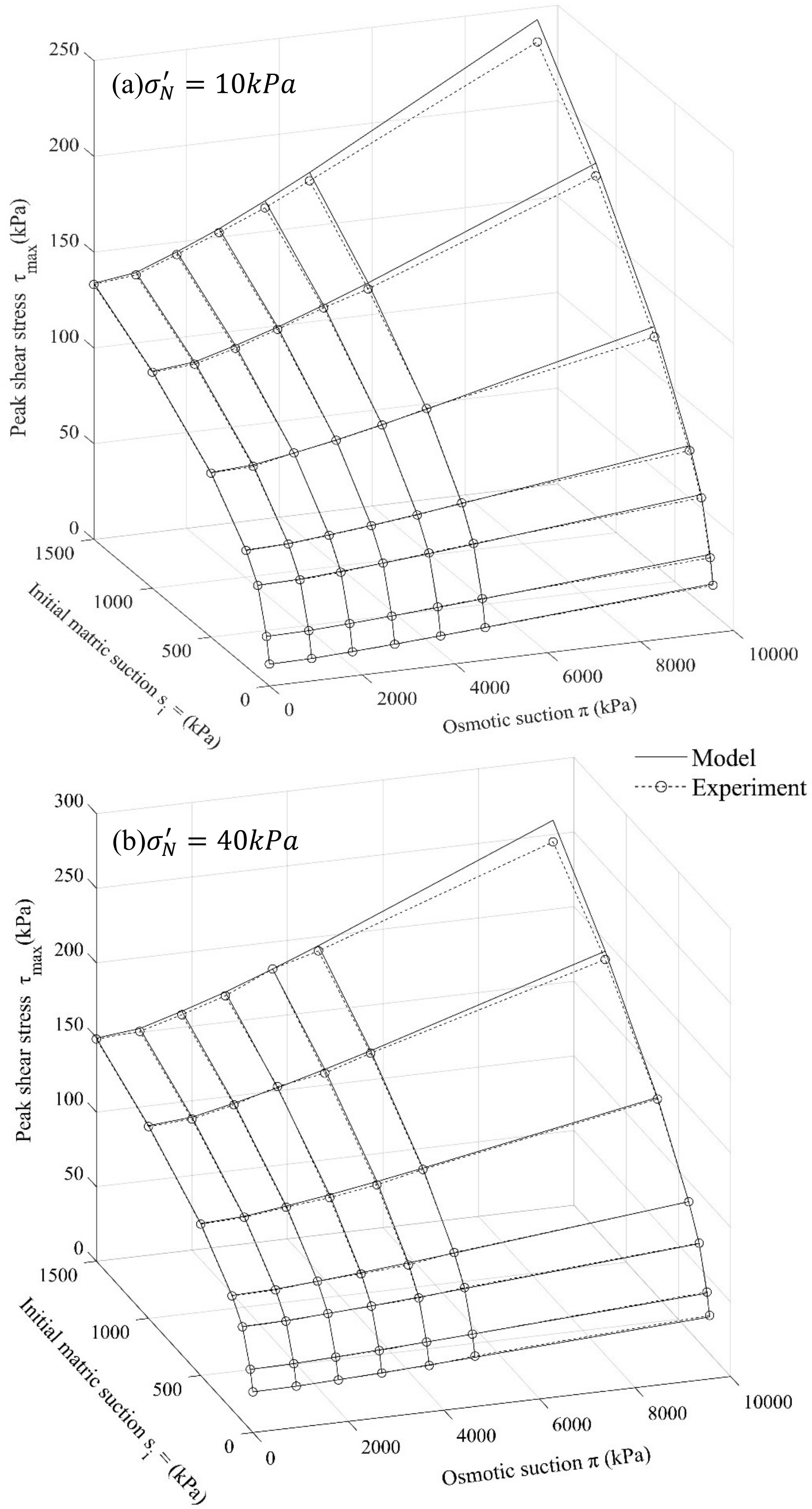
(a)$\sigma'_N = 10kPa$
(b)$\sigma'_N = 40kPa$
Peak shear stress $\tau_{max}$(kPa)
Initial matric suction $s_i$ = (kPa)
Osmotic suction π (kPa)
Model
Experiment

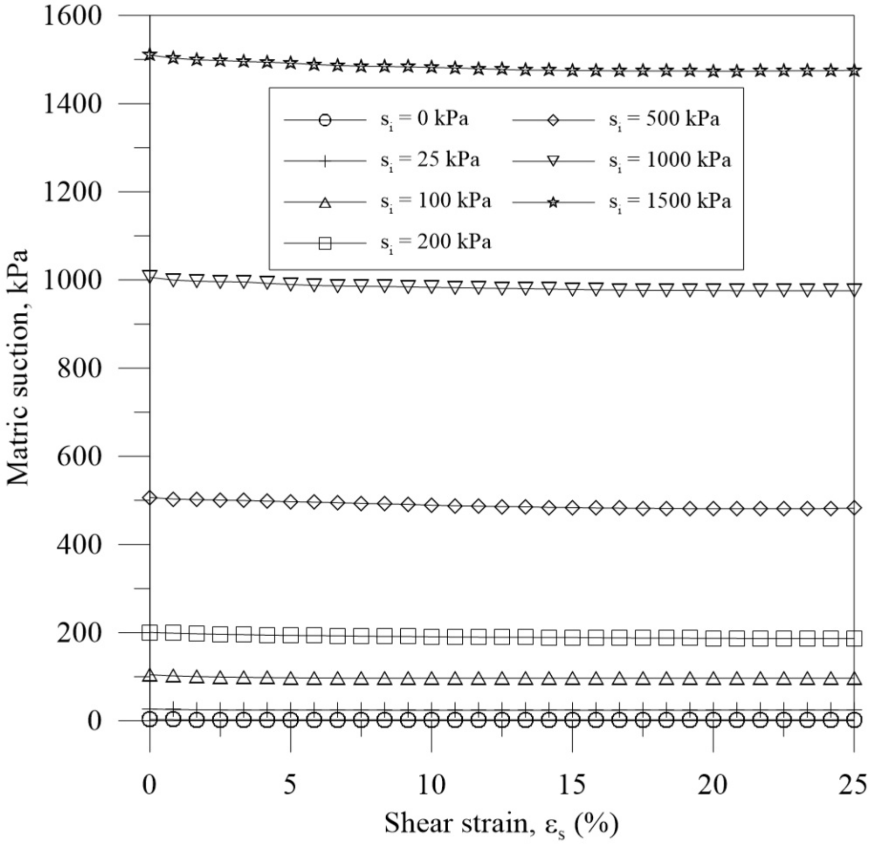

Matric suction, kPa
Shear strain, $\varepsilon_s$ (%)
$s_i$ = 0 kPa
$s_i$ = 25 kPa
$s_i$ = 100 kPa
$s_i$ = 200 kPa
$s_i$ = 500 kPa
$s_i$ = 1000 kPa
$s_i$ = 1500 kPa
0
200
400
600
800
1000
1200
1400
1600
5
10
15
20
25